

# Geophysical Research Letters®



## RESEARCH LETTER

10.1029/2022GL102229

### Key Points:

- $\delta D_p$  at each site continuously decreases in May–September and amplitude of decreasing trends gradually strengthens from south to north
- Upstream water vapor isotope properties shape the continuous decreasing trends of downstream  $\delta D_p$
- Upstream vertical air motions and topographic relief magnify the amplitude of the decreasing trends of the downstream  $\delta D_p$

### Supporting Information:

Supporting Information may be found in the online version of this article.

### Correspondence to:














W. Yu,  
[yuws@itpcas.ac.cn](mailto:yuws@itpcas.ac.cn)

### Citation:

Zhang, J., Yu, W., Lewis, S., Thompson, L. G., Bowen, G. J., Yoshimura, K., et al. (2023). Controls on stable water isotopes in monsoonal precipitation across the Bay of Bengal: Atmosphere and surface analysis. *Geophysical Research Letters*, 50, e2022GL102229. <https://doi.org/10.1029/2022GL102229>

Received 4 DEC 2022  
Accepted 22 FEB 2023

## Controls on Stable Water Isotopes in Monsoonal Precipitation Across the Bay of Bengal: Atmosphere and Surface Analysis

Jingyi Zhang<sup>1</sup> , Wusheng Yu<sup>1</sup> , Stephen Lewis<sup>2</sup> , Lonnie G. Thompson<sup>3</sup> , Gabriel J. Bowen<sup>4</sup> , Kei Yoshimura<sup>5,6</sup> , Alexandre Cauquoin<sup>5</sup> , Martin Werner<sup>7</sup> , Supriyo Chakraborty<sup>8,9</sup> , Zhaowei Jing<sup>10</sup> , Yaoming Ma<sup>1</sup> , Xiaoyu Guo<sup>1</sup> , Baiqing Xu<sup>1</sup>, Guangjian Wu<sup>1</sup> , Rong Guo<sup>1,11</sup>, and Dongmei Qu<sup>1</sup>

<sup>1</sup>State Key Laboratory of Tibetan Plateau Earth System, Environment and Resources (TPESER), Institute of Tibetan Plateau Research, Chinese Academy of Sciences, Beijing, China, <sup>2</sup>Catchment to Reef Research Group, Centre for Tropical Water and Aquatic Ecosystem Research, James Cook University, Townsville, QLD, Australia, <sup>3</sup>Byrd Polar and Climate Research Center, The Ohio State University, Columbus, OH, USA, <sup>4</sup>Department of Geology and Geophysics, University of Utah, Salt Lake City, UT, USA, <sup>5</sup>Institute of Industrial Science, The University of Tokyo, Kashiwa, Japan, <sup>6</sup>Earth Observation Research Center, Japan Aerospace Exploration Agency, Chofu, Japan, <sup>7</sup>Alfred Wegener Institute (AWI), Helmholtz Centre for Polar and Marine Sciences, Bremerhaven, Germany, <sup>8</sup>Indian Institute of Tropical Meteorology, Ministry of Earth Sciences, Pune, India, <sup>9</sup>Department of Atmospheric and Space Sciences, Savitribai Phule Pune University, Pune, India, <sup>10</sup>Function Laboratory for Ocean Dynamics and Climate, Pilot National Laboratory for Marine Science and Technology (QNLN), Qingdao, China, <sup>11</sup>University of Chinese Academy of Sciences, Beijing, China

**Abstract** Stable hydrogen isotopes in monsoonal precipitation ( $\delta D_p$ ) at three sites (Port Blair, Barisal and Darjeeling) reveal the factors governing  $\delta D_p$  variations over a south–north gradient across the Bay of Bengal. We found that the  $\delta D_p$  at each site continuously decreases from May to September and these trends become more pronounced from south to north. The decreasing trends of downstream  $\delta D_p$  closely follow the decreasing trends of upstream stable hydrogen isotopes in water vapor ( $\delta D_v$ ), which indicates that upstream  $\delta D_v$  properties shape initial spatiotemporal patterns of the downstream  $\delta D_p$  (“shaping effect”). Additionally, our results demonstrate that, during moisture transport, upstream vertical air motions (convection and downward motion) and topographic relief magnify the amplitude of the decreasing trends of downstream  $\delta D_p$  (“magnifying effect”). Our findings imply that upstream  $\delta D_v$  properties and relevant atmospheric and topographical conditions along the moisture transport pathway need to be considered collectively to better interpret paleoclimate records.

**Plain Language Summary** The stable isotope records from paleoclimate archives in South Asia have been widely used to indicate the Indian Summer Monsoon (ISM) intensity. However, precipitation stable isotopes across most areas of South Asia show a continuous decrease throughout the monsoon season, which does not track the ISM intensity. Clearly, factors other than the ISM influence the variability of the monsoonal precipitation stable isotopes. Here, we reveal the factors governing the variations of precipitation stable hydrogen isotopes ( $\delta D_p$ ) over a south–north gradient across the Bay of Bengal using the  $\delta D_p$  at three sites (Port Blair, Barisal and Darjeeling). Our results show that a gradual decreasing trend of  $\delta D_p$  from May to September appears at each site. We find that changes in stable hydrogen isotopes in upstream water vapor ( $\delta D_v$ ) largely control the decreasing trends of downstream  $\delta D_p$  from May to September. In addition, we also find that the decreasing trends of  $\delta D_p$  gradually strengthen from south to north. These patterns are attributed to the continuous enhancing influences of upstream vertical air motions, including upstream accumulative convection and downward motion, and topographic relief from south to north. These findings help to explain the inconsistency between the lowest  $\delta D_p$  and the strongest ISM.

## 1. Introduction

The Indian Summer Monsoon (ISM) has a major influence on the regional climate of South Asia and surroundings including the Indian subcontinent and Tibetan Plateau. The history of the ISM across the regions has been reconstructed using stable isotope ( $\delta^{18}O$  and  $\delta D$ ) paleoclimate records derived from speleothems (Sinha et al., 2015), tree rings (Xu et al., 2018), ice cores (Thompson et al., 2000), and deep-sea sediment cores (Rashid et al., 2007). The low/high  $\delta^{18}O$  values in these paleoclimate records were thought to reflect low/high paleo- $\delta^{18}O_p$  values ( $\delta^{18}O$  of precipitation) driven by strong/weak ISM (Joshi et al., 2017). However, recent studies have questioned the link

© 2023. The Authors.

This is an open access article under the terms of the [Creative Commons Attribution License](https://creativecommons.org/licenses/by/4.0/), which permits use, distribution and reproduction in any medium, provided the original work is properly cited.

between ISM intensity and  $\delta^{18}\text{O}_p$  (Cai & Tian, 2020; Midhun et al., 2018). Specifically,  $\delta^{18}\text{O}_p$  values across most areas of South Asia show a continuous decrease throughout the monsoon season from May to September (Ahmed et al., 2020; Chakraborty et al., 2022; Islam et al., 2021; Jeelani et al., 2018; Tanoue et al., 2018), which does not track ISM intensity (highest in July–August). Hence, factors other than the ISM appear to influence the variability of stable isotopes across South Asia in the monsoon season. A systematic investigation to unravel these additional influences is then necessary.

The cause of the continuous decrease of  $\delta^{18}\text{O}_p$  from May to September in South Asia has been subject to increasing investigations (Breitenbach et al., 2010; Midhun et al., 2018; Oza et al., 2020) and competing hypotheses have emerged in the literature. Some researchers have proposed that the shift of moisture sources from the west Arabian Sea (AS) to the east Bay of Bengal (BoB) is the major factor governing the continuous decrease of  $\delta^{18}\text{O}_p$  from May to September in the central and northern part of the Indian subcontinent (Lekshmy et al., 2018; Midhun et al., 2018; Sengupta & Sarkar, 2006). But the reason for the similar trend of  $\delta^{18}\text{O}_p$  in other areas, including the head BoB, is still unclear. Cai and Tian (2020) put forward that moisture transport from the east causes decreased  $\delta^{18}\text{O}_p$  at the head BoB during the post-monsoon period (October), but this hypothesis cannot explain the continuous decrease of  $\delta^{18}\text{O}_p$  in this area throughout the monsoon season. While the upstream moisture sources are widely regarded as a key influence on the downstream  $\delta^{18}\text{O}_p$  (Bhattacharya et al., 2003; Ichiyangi et al., 2005; Kathayat et al., 2021; Midhun et al., 2018; Ren et al., 2021), the effects of upstream water vapor stable isotopes on the changes of the downstream precipitation stable isotopes have received scant attention. These issues motivate the need to better understand the role of the upstream water vapor stable isotopes on the downstream precipitation stable isotopes in South Asia, especially in the area across the BoB.

Vertical air motions have an important influence on the transport of moisture in the South Asia region. Several studies have demonstrated that strong convection, which prevails vertical upward motion and frequently occurs in the low latitudes during the monsoon season (He et al., 2021; Kurita, 2013), can contribute to the relatively low  $\delta^{18}\text{O}_p$  in South Asia (Ansari et al., 2020; Chakraborty et al., 2016; Islam et al., 2021; Lekshmy et al., 2014; Permana et al., 2016). Recently, upstream accumulative convection has been suggested to help explain  $\delta^{18}\text{O}_p$  variations in this region during the monsoon season (Cai & Tian, 2020; Midhun et al., 2018). However, how the upstream accumulative convection cause downstream precipitation stable isotopes to change along a south-north transect through South Asia from May to September is still unknown. Moreover, except for convection, few studies have discussed the contribution of the downward motion on the decrease of precipitation stable isotopes across the BoB. These knowledge gaps drive a further need to examine the influence of vertical air motions on the downstream precipitation stable isotopes.

While many of the studies described above have addressed possible factors that influence the changes of the monsoonal precipitation stable isotopes from the perspective of dynamic processes in the atmosphere (such as monsoon, moisture transport, convection, etc.), there has been limited attention on the additional influence of surface topography on precipitation stable isotopes in South Asia. Topographic differences not only can lead to spatial heterogeneity of precipitation amount, they may also cause variability in precipitation stable isotopes across the area. In this regard, a systematic investigation that couples the influence of upstream atmospheric dynamic processes with surface topographic relief on the downstream precipitation stable isotopes is required to resolve the variability of precipitation stable isotopes in South Asia throughout the monsoon season.

This study analyzes the spatiotemporal patterns of precipitation  $\delta D$  ( $\delta D_p$ ) from May to September on a south-north transect across the BoB. Our aim is to identify the main factors that influence  $\delta D_p$  variability based on both atmospheric and land surface analyses. First, we verify the crucial influences of upstream atmospheric water vapor  $\delta D$  ( $\delta D_v$ ) properties on the spatiotemporal patterns of downstream  $\delta D_p$ . Second, we determine the role of upstream vertical air motions on the downstream  $\delta D_p$ . Third, we examine the influence of topographic relief of the landscape during the moisture transport process on  $\delta D_p$  variability. Finally, we discuss the coupled influences of the three factors mentioned above on the spatiotemporal patterns of  $\delta D_p$  across the south-north study sites.

## 2. Materials and Methods

### 2.1. Study Sites and Stable Isotope Data

To capture  $\delta D_p$  variability across the South Asia region, three study sites covering a south-north transect across the BoB were selected which include Port Blair, Barisal, and Darjeeling (Figure 1a; see Text S1 and Table S1 in

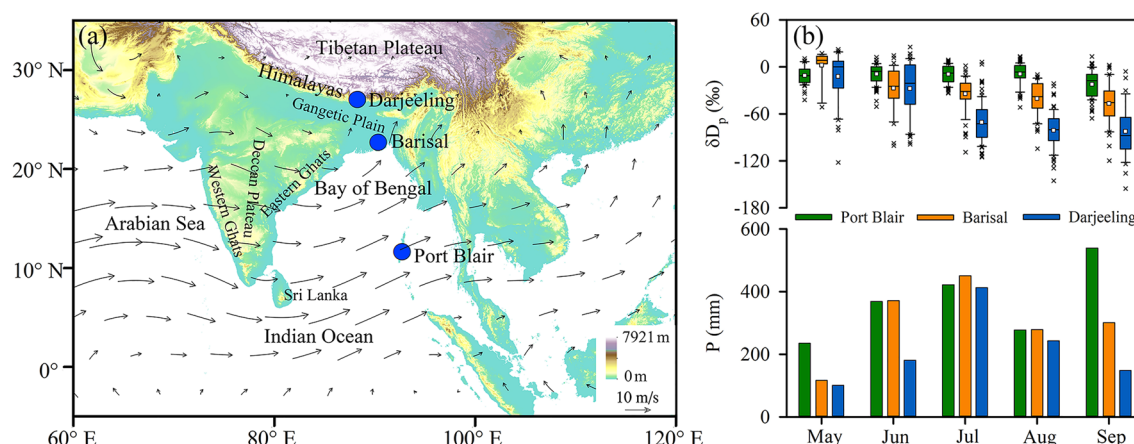


**Figure 1.** (a) Map of South Asia with the locations of our three sites of interest. The climatological wind vectors at the 850 hPa level during May to September (arrows, units: m/s, data sources: ERA5) are also shown. (b) Temporal variations of  $\delta D_p$  (boxplots) and precipitation amount (histograms) at the three study sites from May to September. In the boxplots, the lower and upper limits of the whiskers indicate the minima and maxima; the lower and upper limits of the boxes indicate the 25th and 75th percentiles; the horizontal black lines in the boxes indicate the median; the white squares in the boxes represent the mean; and crosses denote outliers.

Supporting Information S1 for details). The daily  $\delta D_p$  observations from the sites of Port Blair and Barisal and the site of Darjeeling were obtained from Munksgaard et al. (2019) and this study, respectively (Text S2 and Table S1 in Supporting Information S1). The  $\delta D_v$  values were retrieved from the Tropospheric Emission Spectrometer (TES) Level 2 product (version 7) onboard NASA's Aura satellite (Text S2 in Supporting Information S1).

In addition, we used  $\delta D_p$  and  $\delta D_v$  outputs from two isotope-enabled Atmosphere General Circulation Models (AGCMs): ECHAM6-wiso (Cauquoin et al., 2019; Cauquoin & Werner, 2021) and IsoGSM2 (Yoshimura et al., 2008) (see Text S2 in Supporting Information S1 for the details on models and simulation setups). Both models reproduce fairly well the temporal variations of precipitation isotope in-situ measurements and TES isotope data at each site (Figures S1, S2, and Text S2 in Supporting Information S1).

## 2.2. HYSPLIT Model Moisture Sources Diagnosis

We identified the air mass back trajectories using the Hybrid Single Particle Lagrangian Integrated Trajectory (HYSPLIT) model version 4.0 (Stein et al., 2015). Detailed descriptions on the moisture source diagnostic method can be found in Text S4 in Supporting Information S1 (Cai et al., 2018; Zhang et al., 2021). To investigate the influences of upstream accumulative convection on  $\delta D_p$ , we traced changes in precipitation amount and outgoing longwave radiation (OLR) (Text S3 in Supporting Information S1) along the back trajectories using the HYSPLIT model.

## 3. Results

Figure 1 shows the monthly changes in observed  $\delta D_p$  at the three study sites from May to September. At Port Blair, the mean monthly  $\delta D_p$  values fluctuate slightly from May to August (between  $-8.90$  and  $-10.91$ ‰) and decrease further in September ( $-22.18$ ‰) (Figure 1b). At Barisal and Darjeeling, the highest mean monthly  $\delta D_p$  values occur in May and the lowest values appear in September (Figure 1b). Overall, there is a continuous decreasing trend from May to September across all sites (Figure 1b).

From south to north, the decrease in the amplitude of  $\delta D_p$  values over the May–September period gradually strengthens, with slopes of  $-2.26$ ,  $-11.09$ , and  $-19.36$ , for Port Blair, Barisal, and Darjeeling, respectively (Figure 1b). Indeed, the mean  $\delta D_p$  values at Port Blair, Barisal, and Darjeeling for the month of May are relatively high ( $-10.91$ ,  $2.17$ , and  $-12.12$ ‰, respectively), but decrease distinctly from south to north in September ( $-22.18$ ,  $-46.71$ , and  $-82.20$ ‰, respectively) (Figure 1b).

The monthly  $\delta D_p$  variability from May to September is not consistent with the precipitation amount variability at these sites (Figure 1b). Moreover, the negative correlations between daily precipitation amount and  $\delta D_p$  are

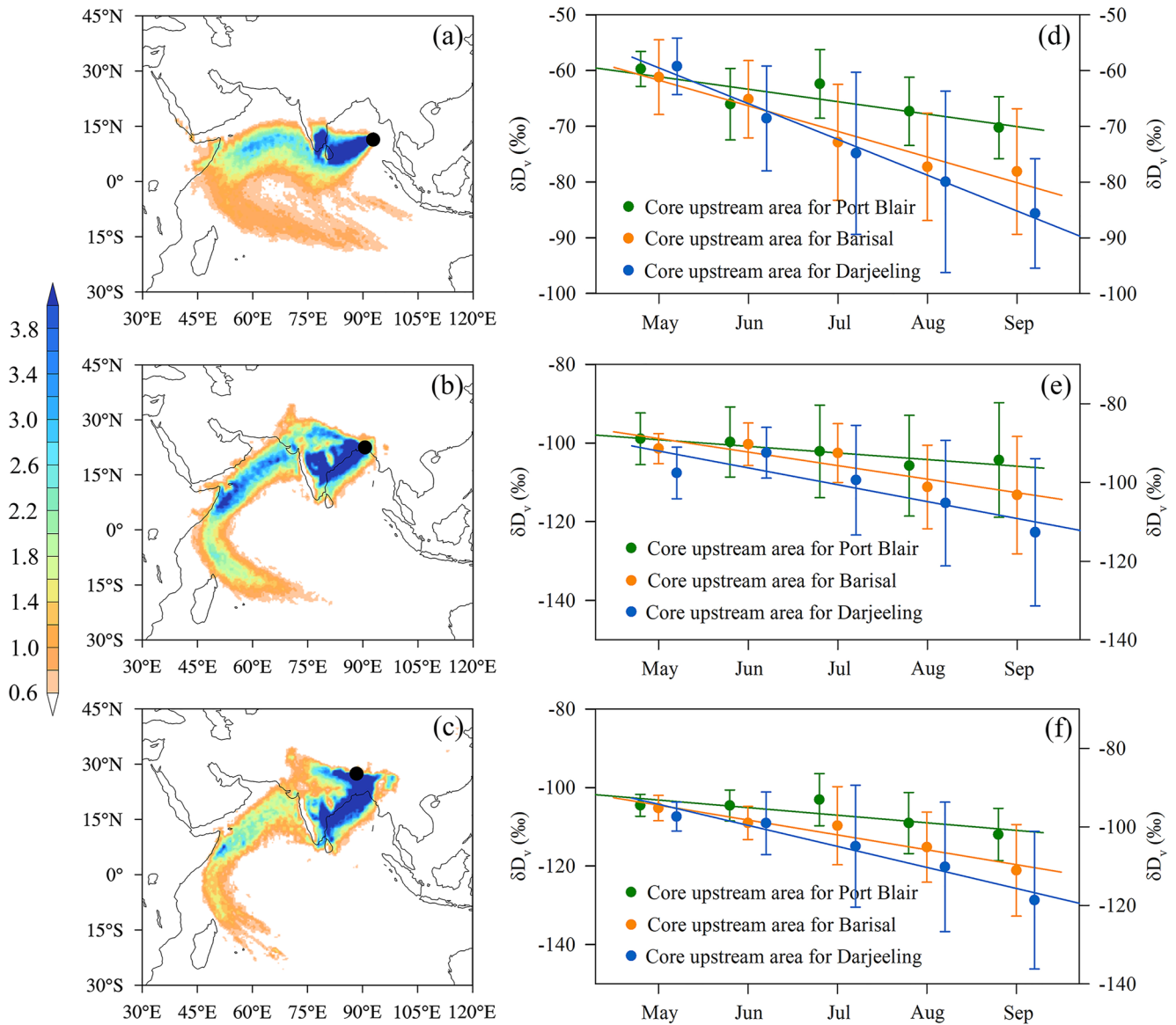


**Figure 2.** (a–c) Spatial distribution of mean fractional moisture contribution ( $10^{-4}$ ) during May–September for Port Blair (a), Barisal (b), and Darjeeling (c). The black dots in (a–c) indicate the location of the study sites. (d–f) Temporal variations of specific humidity weighted average  $\delta D_v$  over 1,000–500 hPa in the core upstream areas for the three downstream study sites from TES (d), ECHAM6-wiso (e), and IsoGSM2 (f). The dots in (d–f) indicate the mean and standard deviations are marked by error bars. The left (right) y-axis in (d–f) represents the  $\delta D_v$  in the core upstream areas for Port Blair (Barisal and Darjeeling).

weak at all three sites (correlation coefficients are  $-0.26$ ,  $-0.27$ , and  $-0.24$  from south to north) (Figure S6 in Supporting Information S1). Therefore, the  $\delta D_p$  variations at the three sites do not appear to be influenced by local precipitation amount only.

## 4. Discussion

### 4.1. Influence of Upstream $\delta D_v$ Properties on the Downstream $\delta D_p$

To examine the influence of upstream  $\delta D_v$  properties on the downstream  $\delta D_p$  within the atmosphere, the total upstream moisture contribution areas are first diagnosed using the moisture source diagnostic method (Text S4 in Supporting Information S1). Our results show that, under the influence of the strong ISM, moisture originating from the Indian Ocean (IO) travels across the AS, Indian subcontinent, and BoB and reaches the study area (Figures 2a–2c). That is, the moisture contribution to the three downstream sites is mainly derived from the



regions at the west and southwest of the study sites (Figures 2a–2c). This result is different from previous studies focusing on central and northern India (dual moisture sources from the regions to the east and west of the study area) (Midhun et al., 2018; Sengupta & Sarkar, 2006). Hence, we propose that the moisture contribution from the east cannot explain the continuous decrease of  $\delta D_p$  over the monsoon period in our study area. We now explore the possible factors in the upstream moisture contribution areas to the west and southwest of the study sites that cause the downstream  $\delta D_p$  to decrease.

As the total upstream moisture contribution areas for each site vary for each month, we investigated the multi-monthly mean fractional moisture contributions during May, June, July, August, and September separately (Figures S7–S9 in Supporting Information S1). The major upstream moisture contribution areas to the downstream study sites are highlighted in Figures S7–S9 in Supporting Information S1 (marked by diagonal lines) and have been defined as core upstream moisture contribution areas (hereafter called “core upstream areas”). To characterize the  $\delta D_v$  properties in the three core upstream areas for the three downstream study sites, we plotted the multi-monthly mean  $\delta D_v$  from TES over the 1,000–510 hPa pressure range (Figure 2d). The results show that from May to September, the  $\delta D_v$  from TES in the core upstream areas for Port Blair, Barisal, and Darjeeling continuously decreases from  $-59.71$  to  $-70.24\text{‰}$ , from  $-61.19$  to  $-78.11\text{‰}$ , and from  $-59.22$  to  $-85.63\text{‰}$ , with slopes of  $-2.23$ ,  $-4.60$ , and  $-6.42$ , respectively (Figure 2d). The modeled  $\delta D_v$  values from ECHAM6-wiso and IsoGSM2 in the core upstream areas show the similar decreasing patterns from May to September at each site. With ECHAM6-wiso, the slopes of  $-1.69$ ,  $-3.44$ , and  $-4.30$  for Port Blair, Barisal, and Darjeeling are found, respectively (Figure 2e). With IsoGSM2, these slopes are equal to  $-1.94$ ,  $-3.79$ , and  $-5.37$  for the three sites, respectively (Figure 2f). So, the decreasing trends of the upstream  $\delta D_v$  match the decreasing trends of downstream  $\delta D_p$  at the three study sites (Figures 2d–2f, Figure S10 in Supporting Information S1). These results demonstrate that the  $\delta D_v$  properties in the core upstream areas considerably influence the downstream  $\delta D_p$  across the BoB. Our findings are also supported by the results from Sinha and Chakraborty (2020), who found that the  $\delta D_v$  variations calculated by a Craig-Gordon Model in the source region are consistent with the  $\delta D_p$  changes at Port Blair.

#### 4.2. Influence of Upstream Vertical Air Motions on the Downstream $\delta D_p$

The effects of upstream vertical air motions (i.e., the upstream accumulative convection and downward motion) on the downstream  $\delta D_p$  are discussed in this section. The upstream accumulative precipitation and average OLR are widely used to assess the influence of the upstream accumulative convection on the downstream  $\delta D_p$  in the low latitudes (Cai & Tian, 2020; Vimeux et al., 2011; Zwart et al., 2016). In this study, we analyzed the changes of precipitation amount and OLR along the back trajectories, and calculated the correlations between the daily  $\delta D_p$  at the three downstream study sites and the upstream accumulative precipitation amount and upstream average OLR (Figure S11 in Supporting Information S1). These results indicate that the influence of upstream accumulative convection on the downstream  $\delta D_p$  mainly occurs over the initial four days (Figure S11 and Text S5 in Supporting Information S1).

To focus on the influence of upstream accumulative convection and the downward motion on the downstream  $\delta D_p$ , we then examine the variations of average OLR along the back trajectories over the initial 4 days from May to September (Figures 3a–3c). We then analyze the vertical profiles of the meridional average vertical velocity anomalies and the  $\delta D_v$  anomalies (values in each month subtracted by the mean values during May–September) from May to September across the core upstream areas for each site (Figures 3d–3r, Figures S12–S14 in Supporting Information S1). For Port Blair, the variations of the initial four-day average upstream OLR are subtle during the May–September period (fluctuate in  $220$ – $240$   $\text{W/m}^2$ ) (Figure 3a). In addition, the upstream vertical velocity anomalies have no obvious changes during the monsoon period for Port Blair (Figures 3d, 3g, 3j, 3m and 3p). These results are consistent with the limited fluctuations of downstream  $\delta D_p$  at this site (Figure 1b). Those indicate that the relatively small changes in the upstream vertical air motions (upstream accumulative convection and downward motion) contribute to the slight fluctuations of downstream  $\delta D_p$  at Port Blair over this period.

For Barisal, the initial four-day average upstream OLR values are relatively high in May ( $>260$   $\text{W/m}^2$ ) (Figure 3b), and the corresponding upstream vertical velocities show positive anomalies (Figure 3e), which indicate very weak convection and abnormal downward motion. Interestingly, the upstream  $\delta D_v$  values show positive anomalies in the  $700$ – $500$  hPa levels in May (Figure 3e, Figures S13f, S13k and S13p in Supporting Information S1). In this case, the abnormal downward motion carries the water vapor with relatively high  $\delta D_v$  values

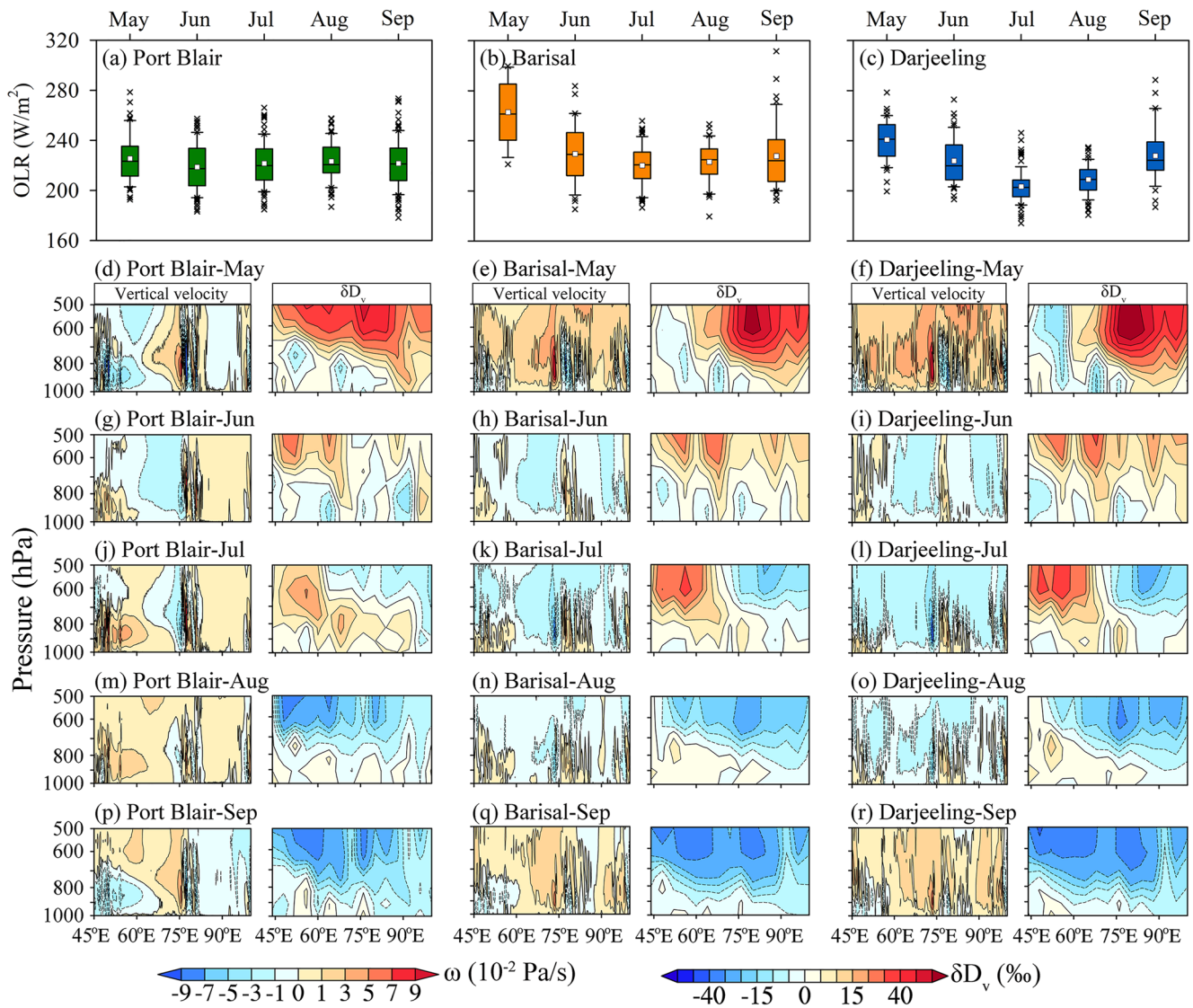


**Figure 3.** (a–c) Temporal variations of the upstream average outgoing longwave radiation (OLR) along the back trajectories over the initial four days for Port Blair (a), Barisal (b), and Darjeeling (c) during May–September; (d–r) Vertical profiles of meridional average vertical velocity ( $\omega$ ) anomalies from ERA5 reanalysis data and  $\delta D_v$  anomalies from TES across the core upstream areas for Port Blair (d, g, j, m, p), Barisal (e, h, k, n, q), and Darjeeling (f, i, l, o, r) during May–September. The latitude ranges for calculating the meridional average in (d–r) are 5–13°N for Port Blair, 5–26°N for Barisal, and 10–28°N for Darjeeling, which are identified based on the latitude ranges of the core upstream areas for each site. Negative and positive anomaly values for  $\omega$  indicate upward and downward motion, respectively.

from the 700–500 hPa levels to the higher 1,000–700 hPa pressure levels, and then the relatively high  $\delta D_v$  can be transported to Barisal. This process results in relatively high  $\delta D_p$  values at this site in May (Figure 1b). In the June–August period, the initial four-day average upstream OLR values significantly decrease ( $<230 \text{ W/m}^2$ ) (Figure 3b), which implies that upstream accumulative convection become strong during this period. This result is confirmed by the negative anomalies of upstream vertical velocities in June–August (Figures 3h, 3k, and 3n). Therefore, the enhanced upstream accumulative convection corresponds to the decreases of the downstream  $\delta D_p$  between June and August at Barisal (Figure 1b). Nevertheless, in September, the upstream vertical velocity turns to positive anomalies (Figure 3q). The result reflects that abnormal downward motion prevails during September. Unlike in May, the corresponding upstream  $\delta D_v$  presents clear negative anomalies in the 700–500 hPa levels in September (Figure 3q, Figures S13j, S13o, and S13t in Supporting Information S1). Thus, more water vapor with relatively low  $\delta D_v$  values in the 700–500 hPa levels can be carried lower in altitude to the 1,000–700 hPa levels by the abnormal downward motion and be transported to Barisal, contributing the lower  $\delta D_p$  values in September. These processes explain the continuous decrease of  $\delta D_p$  in September at Barisal. In short, both the

enhanced upstream accumulative convection during June–August and the abnormal downward motion in May and September influences the downstream  $\delta D_p$  values at Barisal. Moreover, compared with Port Blair, the influences of upstream vertical air motions on the downstream  $\delta D_p$  from May to September are more important at Barisal, which results in a larger amplitude of the  $\delta D_p$  decreasing trend at this site (Figure 3 and Figures S12, S13 in Supporting Information S1).

For Darjeeling, the pattern of the initial four-day average upstream OLR, upstream vertical velocity anomalies, and upstream  $\delta D_v$  anomalies are fairly consistent with the ones at Barisal (Figure 3 and Figures S13, S14 in Supporting Information S1), all of which play an important role in the continuous decrease of downstream  $\delta D_p$  values at this site. However, compared with Barisal, we find that the initial four-day average upstream OLR values for Darjeeling are lower during June–August (Figures 3b and 3c), and the negative vertical velocity anomalies are more pronounced during June–August at the site (Figures 3h, 3i, 3k, 3l, 3n, and 3o). Thus, stronger upstream accumulative convection leads to the more significant decrease of downstream  $\delta D_p$  values during June–August at Darjeeling relative to Barisal (Figure 1b). In September, the positive vertical velocity anomalies and negative  $\delta D_v$  anomalies at the 700–500 hPa levels are more pronounced in the upstream moisture contribution areas for Darjeeling than those for Barisal (Figures 3q and 3r, Figures S13j, S13o, S13t, S14j, S14o, and S14t in Supporting Information S1). Thus, the impact of downward motion on the downstream  $\delta D_p$  in September is more important at Darjeeling than at Barisal, corresponding to the lower  $\delta D_p$  values at Darjeeling (Figure 1b). That is, the larger decreasing amplitude of the  $\delta D_p$  values from June to September at Darjeeling than at Barisal is attributed to the greater influence of the upstream vertical air motions at Darjeeling.

Overall, the influence of upstream vertical air motions on the downstream  $\delta D_p$  values gradually strengthens from south to north during the monsoon season, and those are responsible for the spatiotemporal patterns of downstream  $\delta D_p$  at the three sites.

### 4.3. Influence of Topographic Relief on the Downstream $\delta D_p$

The topographic relief of the landscape can affect precipitation amount and the associated  $\delta D_p$  (Rahul et al., 2016; Yu et al., 2014, 2021). To investigate this influence on the  $\delta D$  signal, we used the averaged back trajectories of precipitation days during May–September, extending northward and southward  $2.5^\circ$  of latitude, to identify the main moisture channels (Figure S15 in Supporting Information S1). The topographic relief was extracted along these main moisture channels (Figure 4). As ECHAM6-wiso has a relatively higher spatial resolution, allowing a better representation of topography effects on modeled climate isotope variables, we use the outputs of this model combined with the observed  $\delta D_p$  from the Global Network of Isotopes in Precipitation (GNIP) for the analysis below. We find similar results using the outputs from IsoGSM2 (Figure S16 in Supporting Information S1).

For Port Blair, the main moisture channel extends from the oceans, and only travels to the island of Sri Lanka across a relatively low altitude (Figure 4a, Figure S15 in Supporting Information S1). As a result, the  $\delta D_v$  and  $\delta D_p$  only slight decrease from the west coast of Sri Lanka (Colombo) to Port Blair (modeled  $\delta D_v$ , modeled  $\delta D_p$ , and observed  $\delta D_p$  decreases by 15.39, 12.78, and 3.07‰ respectively) (Figure 4a). Thus, the topographic influence on the  $\delta D_v$  and  $\delta D_p$  values from the IO to Port Blair is relatively weak (Figure 4a).

For Barisal, the ISM-driven moisture originating from the AS is transported from west to east, and the observed  $\delta D_p$  values (−2.90‰) as well as the modeled  $\delta D_v$  (−88.37‰) and  $\delta D_p$  (−2.78‰) values on the western coast of the Indian subcontinent (Mumbai) are relatively high due to the flat topographic relief (Figure 4b). However, when this moisture is transported across the Western Ghats and Deccan Plateau, it is uplifted to higher altitudes (Figure 4b). This uplift influence in combination with rainout results in a decrease in  $\delta D_v$  (the modeled ECHAM6-wiso  $\delta D_v$  value decreases from −88.37‰ at Mumbai to −93.20‰ at Hyderabad) and the subsequent  $\delta D_p$  values (from Mumbai to Hyderabad, the modeled and observed  $\delta D_p$  values decrease from −2.78 to −11.57‰ and from −2.90 to −10.88‰, respectively) (Figure 4b). Eventually, the residual moisture travels through the Eastern Ghats, the BoB and the Gangetic Plain to reach the downstream site of Barisal, where the corresponding modeled  $\delta D_v$ , subsequent modeled  $\delta D_p$  and observed  $\delta D_p$  decrease to −107.71, −30.79 and −29.28‰, respectively (Figure 4b). In this process, the modeled  $\delta D_p$  changes also capture the influence of topographic relief (Figure 4b). In comparison to Port Blair, the elevated and complex topography over the moisture transport pathway to Barisal contributes to the relatively larger decreases of  $\delta D_v$  and  $\delta D_p$  at this site (Figures 4a and 4b).

Similar to Barisal, the main moisture channel for Darjeeling also extends over a continuous and wide region of mountains and plateaus (Figure 4c, Figure S15 in Supporting Information S1). Consequently, the  $\delta D_v$  and  $\delta D_p$

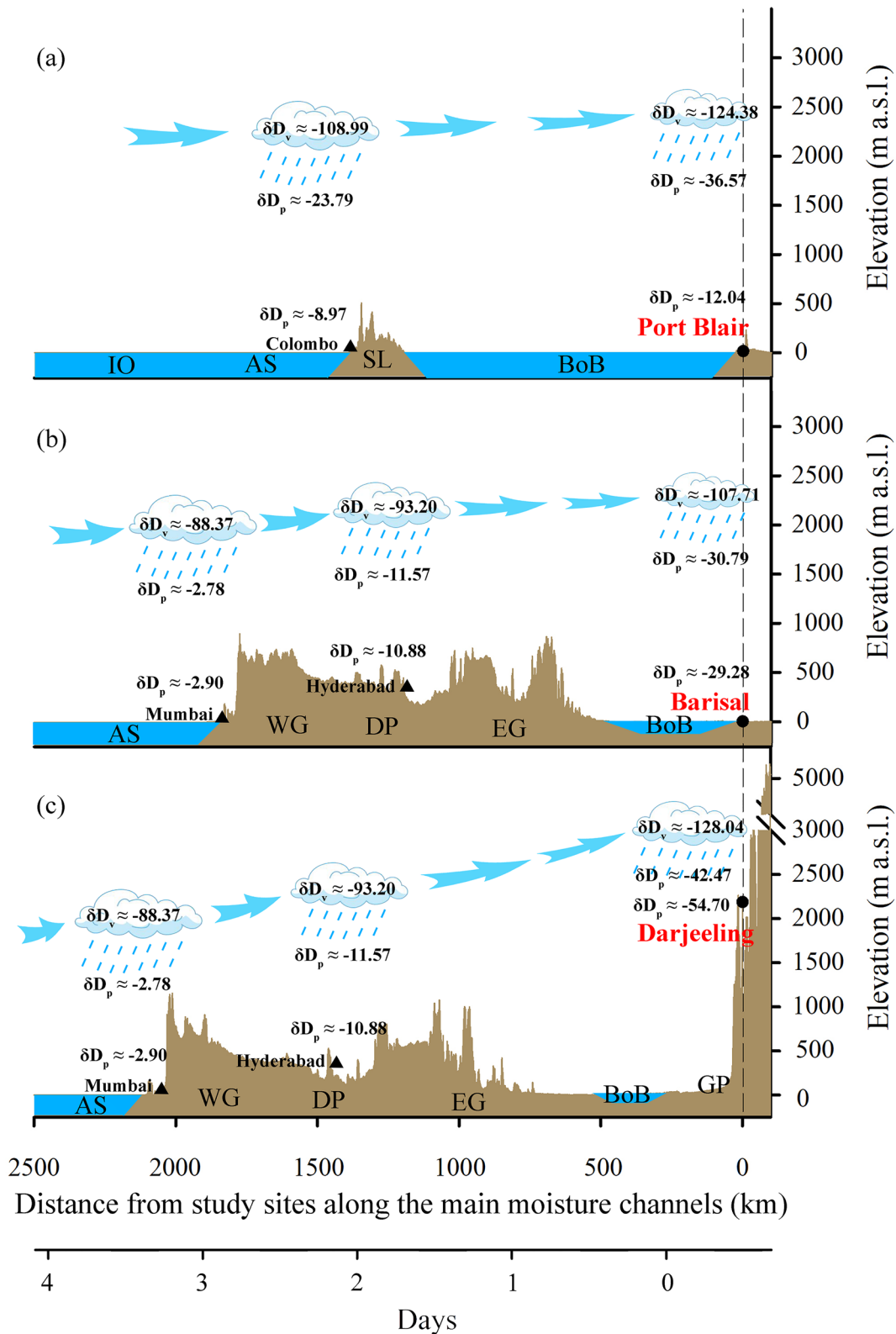


**Figure 4.** Schematic diagram of moisture transport along the main moisture channels for Port Blair (a), Barisal (b), and Darjeeling (c). Brown shading indicates topographic relief (SL: Sri Lanka; WG: Western Ghats; DP: Deccan Plateau; EG: Eastern Ghats; GP: Gangetic Plain), and blue shading indicates oceans. The black dots highlight the locations of the three study sites, and the black triangles represent the locations of the upstream sites. The modeled  $\delta D_v$  and  $\delta D_p$  values (‰) were obtained from ECHAM6-wiso and are shown in and under the cloud respectively. The observed  $\delta D_p$  values (‰) were obtained from the GNIP and are shown near the site's labels.



values over the moisture channels for Darjeeling also experience similar decreases (Figure 4c). Unlike Barisal which is located on the coastal plain with a very low altitude of 7 m a.s.l. (Figure 4b and Table S1 in Supporting Information S1), Darjeeling is located on the southern foothills of the Himalayas with an altitude of 2,042 m a.s.l. (Figure 4c and Table S1 in Supporting Information S1). Due to this higher altitude, the moisture from the upstream sources transported to Darjeeling undergoes relatively stronger rainout and the corresponding  $\delta D_v$  and  $\delta D_p$  values become lower. Other evidence comes from the comparison between the Darjeeling and Tezpur sites lying at similar latitude (Chakraborty et al., 2022). The altitude of Darjeeling is significantly higher than that of Tezpur (48 m a.s.l., see Table S2 in Supporting Information S1 for details), as a result, the average observed  $\delta D_p$  values ( $-54.70\text{‰}$ ) during the monsoon season at Darjeeling are lower than that at Tezpur ( $-39.77\text{‰}$ ). The comparison further demonstrates that topographic changes can affect the  $\delta D_p$  values. We conclude that the topographic relief influences the variations of downstream  $\delta D_p$  values at the three sites, and this influence gradually becomes stronger from south to north.

#### 4.4. Coupled Influences of Atmosphere and Surface Factors on the Downstream $\delta D_p$

We find that the decreasing trends of upstream  $\delta D_v$  shape the decreasing patterns of the downstream  $\delta D_p$  from May to September (Figures 2d–2f). While the amplitude of the decreasing trends of upstream  $\delta D_v$  for Port Blair is similar to the downstream  $\delta D_p$  values (Figures 2d–2f), the amplitudes of the decreasing trends of upstream  $\delta D_v$  for both Barisal and Darjeeling are considerably smaller than the corresponding downstream  $\delta D_p$  values (Figures 2d–2f, Figure S10 in Supporting Information S1). The decreasing trends of upstream  $\delta D_v$  approach those of the downstream  $\delta D_p$  when the added influences of the upstream vertical air motions and topographic relief are taken into account.

Specifically for Port Blair, the subtle variations of upstream vertical air motions (upstream accumulative convection and downward motion) from May to September coupled with the low topographic relief along the moisture transport pathway (Figures 3 and 4a) results in a slight decreasing trend of the downstream  $\delta D_p$  at this site that closely inherits the upstream  $\delta D_v$  signature (Figures 1b, 2d–2f, Figure S10 in Supporting Information S1). For Barisal, the relatively larger influences of both the upstream accumulative convection during June–August and downward motion anomalies in May and September (Figure 3) compared to those for Port Blair cause the downstream  $\delta D_p$  at this site to decrease over this period (Figure 1b, Figure S10 in Supporting Information S1). Importantly, the increasing moisture transported from the IO and AS during the June–September period (i.e., compared with May) (Figure S8 in Supporting Information S1) is more strongly influenced by the elevated topography along the transport pathway (especially at the Western Ghats and Deccan Plateau). As a consequence, the downstream  $\delta D_p$  at Barisal decreases further during June–September and results in a greater increase in the amplitude of the decreasing trend of the downstream  $\delta D_p$  compared to Port Blair (Figure 1b, Figure S10 in Supporting Information S1). While the core upstream area and transport pathway for Darjeeling are similar to Barisal (Figures S8, S9, and S15 in Supporting Information S1), the upstream accumulative convection is stronger during June–August, and the downward motion and negative  $\delta D_v$  anomalies are more pronounced in September for Darjeeling than for Barisal (Figure 3, Figures S13 and S14 in Supporting Information S1). Those increase significantly the amplitude of the decreasing trend of the downstream  $\delta D_p$  at Darjeeling relative to Barisal. Therefore, the most significant effects of upstream vertical air motions during June–September combined with the elevated topographic relief contributes to the largest amplitude of the decreasing trends of the downstream  $\delta D_p$  at Darjeeling compared to the other sites (Figure 1b, Figure S10 in Supporting Information S1).

In summary, the spatiotemporal patterns of the downstream  $\delta D_p$  across the BoB are the result of the coupled influence of atmosphere (upstream  $\delta D_v$  properties and vertical air motions) and surface factors (topographic relief).

## 5. Conclusions

This study investigated the spatiotemporal variations of  $\delta D_p$  at Port Blair, Barisal, and Darjeeling over a south–north transect across the BoB over the May–September period. Our results show that  $\delta D_p$  values at all three sites continuously decrease from May to September, with an amplitude of these decreasing trends smaller in the south and larger in the north. We find that the decreasing trends of upstream  $\delta D_v$  mirror those of downstream  $\delta D_p$  and highlight the “shaping effect” of upstream  $\delta D_v$  properties on the downstream  $\delta D_p$ . The strong

influence of the upstream vertical air motions on the downstream  $\delta D_p$  in May–September for Darjeeling increases the amplitude of the decreasing trend of downstream  $\delta D_p$  throughout the monsoon season. The opposite is true at Port Blair. The topographic relief of the landscape also enhances the spatial variations of the downstream  $\delta D_p$ . Therefore, the combination of the upstream  $\delta D_v$  properties, the upstream vertical air motions, and the topographic relief over the moisture transport pathway collectively drive the spatiotemporal patterns of  $\delta D_p$  at the downstream study sites.

Here we demonstrate why the gradually decreasing trend of  $\delta D_p$  from May to September across the BoB is inconsistent with changes in ISM intensity. We propose that the coupled influences of atmosphere and surface factors on the downstream  $\delta D_p$  changes should be considered in future paleoclimate reconstructions, especially ISM history.

## Data Availability Statement

Sources of the data used in this study are as follows: the observed  $\delta D_p$  data at Darjeeling and Tezpur are available at <https://doi.org/10.6084/m9.figshare.21647123>, and the observed  $\delta D_p$  data at other sites are available from Munksgaard et al. (2019) and the GNIP (<https://nucleus.iaea.org/wiser>, registration is required at this website, and the data can be accessed by clicking “Datasets”). The retrieved  $\delta D_v$  data can be obtained from the satellite data set of the TES onboard NASA’s Aura ([https://search.earthdata.nasa.gov/search/granules?p=C1607585775-LARC!C1607585775-LARC&pg\[1\]\[v\]=t&pg\[1\]\[gsk\]=-start\\_date&q=TL2H2OLN%20V007&qt=2004-08-21T00%3A00%3A00.000Z%2C2018-01-19T23%3A59%3A59.000Z&fi=TES&fl=2%20-%20Geophys.%20Variables%2C%20Sensor%20Coordinates&tl=1669807261.48313!!&lat=0.0703125](https://search.earthdata.nasa.gov/search/granules?p=C1607585775-LARC!C1607585775-LARC&pg[1][v]=t&pg[1][gsk]=-start_date&q=TL2H2OLN%20V007&qt=2004-08-21T00%3A00%3A00.000Z%2C2018-01-19T23%3A59%3A59.000Z&fi=TES&fl=2%20-%20Geophys.%20Variables%2C%20Sensor%20Coordinates&tl=1669807261.48313!!&lat=0.0703125)). The modeled  $\delta D_p$  and  $\delta D_v$  were obtained from the ECHAM6-wiso simulation used in Cauquoin and Werner (2021). The IsoGSM2 outputs (Yoshimura et al., 2008) are available at <https://doi.org/10.6084/m9.figshare.21647123>. The TRMM precipitation data are provided by the NASA Precipitation Measurement Missions (<https://doi.org/10.5067/TRMM/TMPA/3H/7>, the data can be accessed by clicking “Subset/Get Data”). The OLR data are available from the UMD OLR CDR Portal (<http://olr.umd.edu/>). The ERA-Interim reanalysis data are available from <https://apps.ecmwf.int/datasets/data/interim-full-moda/levtype=sfc/>, and ERA5 reanalysis data are available from <https://doi.org/10.24381/cds.6860a573> (Registration is required at the two sites).

## Acknowledgments

This work was funded by the Basic Science Center for Tibetan Plateau Earth System (BSCTPES, NSFC project no. 41988101-03) and the National Natural Science Foundation of China (42171122 and 42071090). Special thanks are given to the editor (Dr. Christopher Cappa) and two anonymous reviewers for their constructive comments.

## References

- Ahmed, N., Kurita, N., Chowdhury, M. A. M., Gao, J., Hassan, S. M. Q., Mannan, M. A., et al. (2020). Atmospheric factors controlling stable isotope variations in modern precipitation of the tropical region of Bangladesh. *Isotopes in Environmental and Health Studies*, 56(3), 220–237. <https://doi.org/10.1080/10256016.2020.1770245>
- Ansari, M. A., Noble, J., Deodhar, A., & Kumar, U. S. (2020). Atmospheric factors controlling the stable isotopes ( $\delta^{18}\text{O}$  and  $\delta^2\text{H}$ ) of the Indian summer monsoon precipitation in a drying region of Eastern India. *Journal of Hydrology*, 584, 124636. <https://doi.org/10.1016/j.jhydrol.2020.124636>
- Bhattacharya, S. K., Froehlich, K., Aggarwal, P. K., & Kulkarni, K. M. (2003). Isotopic variation in Indian Monsoon precipitation: Records from Bombay and New Delhi. *Geophysical Research Letters*, 30(24), 665–678. <https://doi.org/10.1029/2003GL018453>
- Breitenbach, S. F. M., Adkins, J. F., Meyer, H., Marwan, N., Kumar, K. K., & Haug, G. H. (2010). Strong influence of water vapor source dynamics on stable isotopes in precipitation observed in Southern Meghalaya, NE India. *Earth and Planetary Science Letters*, 292(1–2), 212–220. <https://doi.org/10.1016/j.epsl.2010.01.038>
- Cai, Z., & Tian, L. (2020). What causes the postmonsoon  $^{18}\text{O}$  depletion over Bay of Bengal head and beyond? *Geophysical Research Letters*, 47(4). <https://doi.org/10.1029/2020GL086985>
- Cai, Z., Tian, L., & Bowen, G. J. (2018). Spatial-seasonal patterns reveal large-scale atmospheric controls on Asian Monsoon precipitation water isotope ratios. *Earth and Planetary Science Letters*, 503, 158–169. <https://doi.org/10.1016/j.epsl.2018.09.028>
- Cauquoin, A., & Werner, M. (2021). High-resolution nudged isotope modeling with ECHAM6-wiso: Impacts of updated model physics and ERA5 reanalysis data. *Journal of Advances in Modeling Earth Systems*, 13(11). <https://doi.org/10.1029/2021MS002532>
- Cauquoin, A., Werner, M., & Lohmann, G. (2019). Water isotopes—Climate relationships for the mid-Holocene and preindustrial period simulated with an isotope-enabled version of MPI-ESM. *Climate of the Past*, 15(6), 1913–1937. <https://doi.org/10.5194/cp-15-1913-2019>
- Chakraborty, S., Burman, P. K. D., Sarma, D., Sinha, N., Datye, A., Metya, A., et al. (2022). Linkage between precipitation isotopes and biosphere-atmosphere interaction observed in northeast India. *npj Climate and Atmospheric Science*, 5(1), 10. <https://doi.org/10.1038/s41612-022-00231-z>
- Chakraborty, S., Sinha, N., Chattopadhyay, R., Sengupta, S., Mohan, P. M., & Datye, A. (2016). Atmospheric controls on the precipitation isotopes over the Andaman Islands, Bay of Bengal. *Scientific Reports*, 6(1), 19555. <https://doi.org/10.1038/srep19555>
- He, S., Jackisch, D., Samanta, D., Yi, P. K. Y., Liu, G., Wang, X., & Goodkin, N. F. (2021). Understanding tropical convection through triple oxygen isotopes of precipitation from the Maritime Continent. *Journal of Geophysical Research: Atmospheres*, 126(4), e2020JD033418. <https://doi.org/10.1029/2020JD033418>
- Ichiyanagi, K., Yoshimura, K., & Yamanaka, M. D. (2005). Validation of changing water origins over Indochina during the withdrawal of the Asian monsoon using stable isotopes. *Sola*, 1(0), 113–116. <https://doi.org/10.2151/sola.2005-030>
- Islam, M. R., Gao, J., Ahmed, N., Karim, M. M., Bhuiyan, A. Q., Ahsan, A., & Ahmed, S. (2021). Controls on spatiotemporal variations of stable isotopes in precipitation across Bangladesh. *Atmospheric Research*, 247, 105224. <https://doi.org/10.1016/j.atmosres.2020.105224>

- Jeelani, G., Deshpande, R. D., Galkowski, M., & Rozanski, K. (2018). Isotopic composition of daily precipitation along the southern foothills of the Himalayas: Impact of marine and continental sources of atmospheric moisture. *Atmospheric Chemistry and Physics*, 18(12), 8789–8805. <https://doi.org/10.5194/acp-18-8789-2018>
- Joshi, L. M., Kotlia, B. S., Ahmad, S. M., Wu, C.-C., Sanwal, J., Raza, W., et al. (2017). Reconstruction of Indian monsoon precipitation variability between 4.0 and 1.6 ka BP using speleothem  $\delta^{18}\text{O}$  records from the Central Lesser Himalaya, India. *Arabian Journal of Geosciences*, 10(16), 356. <https://doi.org/10.1007/s12517-017-3141-7>
- Kathayat, G., Sinha, A., Tanoue, M., Yoshimura, K., Li, H., Zhang, H., & Cheng, H. (2021). Interannual oxygen isotope variability in Indian summer monsoon precipitation reflects changes in moisture sources. *Communications Earth & Environment*, 2(1), 96. <https://doi.org/10.1038/s43247-021-00165-z>
- Kurita, N. (2013). Water isotopic variability in response to mesoscale convective system over the tropical ocean. *Journal of Geophysical Research: Atmospheres*, 118, 10376–10390. <https://doi.org/10.1002/jgrd.50754>
- Lekshmy, P. R., Midhun, M., & Ramesh, R. (2018). Influence of stratiform clouds on  $\delta\text{D}$  and  $\delta^{18}\text{O}$  of monsoon water vapour and rain at two tropical coastal stations. *Journal of Hydrology*, 563, 354–362. <https://doi.org/10.1016/j.jhydrol.2018.06.001>
- Lekshmy, P. R., Midhun, M., Ramesh, R., & Jani, R. A. (2014).  $^{18}\text{O}$  depletion in monsoon rain relates to large scale organized convection rather than the amount of rainfall. *Scientific Reports*, 4(1), 5661–5665. <https://doi.org/10.1038/srep05661>
- Midhun, M., Lekshmy, P. R., Ramesh, R., Yoshimura, K., Sandeep, K. K., Kumar, S., et al. (2018). The effect of monsoon circulation on the stable isotopic composition of rainfall. *Journal of Geophysical Research: Atmospheres*, 123(10), 5205–5221. <https://doi.org/10.1029/2017JD027427>
- Munksgaard, N. C., Kurita, N., Sánchez-Murillo, R., Ahmed, N., Araguas, L., Balachew, D. L., et al. (2019). Data descriptor: Daily observations of stable isotope ratios of rainfall in the tropics. *Scientific Reports*, 9(1), 1–7. <https://doi.org/10.1038/s41598-019-50973-9>
- Oza, H., Padhya, V., Ganguly, A., Saikranthi, K., Rao, T. N., & Deshpande, R. D. (2020). Hydrometeorological processes in semi-arid western India: Insights from long term isotope record of daily precipitation. *Climate Dynamics*, 54(5–6), 2745–2757. <https://doi.org/10.1007/s00382-020-05136-2>
- Permana, D. S., Thompson, L. G., & Setyadi, G. (2016). Tropical West Pacific moisture dynamics and climate controls on rainfall isotopic ratios in southern Papua, Indonesia. *Journal of Geophysical Research: Atmospheres*, 121(5), 2222–2245. <https://doi.org/10.1002/2015JD023893>
- Rahul, P., Ghosh, P., & Bhattacharya, S. K. (2016). Rainouts over the Arabian Sea and Western Ghats during moisture advection and recycling explain the isotopic composition of Bangalore summer rains. *Journal of Geophysical Research: Atmospheres*, 121(11), 6148–6163. <https://doi.org/10.1002/2015JD024579>
- Rashid, H., Flower, B. P., Poore, R. Z., & Quinn, T. M. (2007). A ~ 25 ka Indian Ocean monsoon variability record from the Andaman Sea. *Quaternary Science Reviews*, 26(19–21), 2586–2597. <https://doi.org/10.1016/j.quascirev.2007.07.002>
- Ren, W., Tian, L., & Shao, L. (2021). Regional moisture sources and Indian summer monsoon (ISM) moisture transport from simultaneous monitoring of precipitation isotopes on the southeastern and northeastern Tibetan Plateau. *Journal of Hydrology*, 601, 126836. <https://doi.org/10.1016/j.jhydrol.2021.126836>
- Sengupta, S., & Sarkar, A. (2006). Stable isotope evidence of dual (Arabian Sea and Bay of Bengal) vapour sources in monsoonal precipitation over north India. *Earth and Planetary Science Letters*, 250(3–4), 511–521. <https://doi.org/10.1016/j.epsl.2006.08.011>
- Sinha, A., Kathayat, G., Cheng, H., Breitenbach, S. F. M., Berkelhammer, M., Mudelsee, M., et al. (2015). Trends and oscillations in the Indian summer monsoon rainfall over the last two millennia. *Nature Communications*, 6(8), 6309. <https://doi.org/10.1038/ncomms7309>
- Sinha, N., & Chakraborty, S. (2020). Isotopic interaction and source moisture control on the isotopic composition of rainfall over the Bay of Bengal. *Atmospheric Research*, 235, 104760. <https://doi.org/10.1016/j.atmosres.2019.104760>
- Stein, A. F., Draxler, R. R., Rolph, G. D., Stunder, B. J. B., Cohen, M. D., & Ngan, F. (2015). NOAA's HYSPLIT atmospheric transport and dispersion modeling system. *Bulletin of the American Meteorological Society*, 96(12), 2059–2077. <https://doi.org/10.1175/BAMS-D-14-00110.1>
- Tanoue, M., Ichinagaki, K., Yoshimura, K., Kiguchi, M., Terao, T., & Hayashi, T. (2018). Seasonal variation in isotopic composition and the origin of precipitation over Bangladesh. *Progress in Earth and Planetary Science*, 5(1), 77. <https://doi.org/10.1186/s40645-018-0231-4>
- Thompson, L. G., Yao, T., Mosley-Thompson, E., Davis, M. E., Henderson, K. A., & Lin, P.-N. (2000). A high-resolution millennial record of the South Asian Monsoon from Himalayan ice cores. *Science*, 289(5486), 1916–1920. <https://doi.org/10.1126/science.289.5486.1916>
- Vimeux, F., Tremoy, G., Risi, C., & Gallaire, R. (2011). A strong control of the South American SeeSaw on the intra-seasonal variability of the isotopic composition of precipitation in the Bolivian Andes. *Earth and Planetary Science Letters*, 307(1–2), 47–58. <https://doi.org/10.1016/j.epsl.2011.04.031>
- Xu, C., Sano, M., Dimri, A. P., Ramesh, R., Nakatsuka, T., Shi, F., & Guo, Z. (2018). Decreasing Indian summer monsoon on the northern Indian sub-continent during the last 180 years: Evidence from five tree-ring cellulose oxygen isotope chronologies. *Climate of the Past*, 14(5), 653–664. <https://doi.org/10.5194/cp-14-653-2018>
- Yoshimura, K., Kanamitsu, M., Noone, D., & Oki, T. (2008). Historical isotope simulation using Reanalysis atmospheric data. *Journal of Geophysical Research*, 113(D19), D19108. <https://doi.org/10.1029/2008JD010074>
- Yu, W., Yao, T., Lewis, S., Tian, L., Ma, Y., Xu, B., & Qu, D. (2014). Stable oxygen isotope differences between the areas to the north and south of Qinling Mountains in China reveal different moisture sources. *International Journal of Climatology*, 34(6), 1760–1772. <https://doi.org/10.1002/joc.3799>
- Yu, W., Yao, T., Thompson, L. G., Jouzel, J., Zhao, H., Xu, B., et al. (2021). Temperature signals of ice core and speleothem isotopic records from Asian monsoon region as indicated by precipitation  $\delta^{18}\text{O}$ . *Earth and Planetary Science Letters*, 554, 116665. <https://doi.org/10.1016/j.epsl.2020.116665>
- Zhang, J., Yu, W., Jing, Z., Lewis, S., Xu, B., Ma, Y., et al. (2021). Coupled effects of moisture transport pathway and convection on stable isotopes in precipitation in East Asia: Implications for paleoclimate reconstruction. *Journal of Climate*, 34(24), 9811–9822. <https://doi.org/10.1175/JCLI-D-21-0271.1>
- Zwart, C., Munksgaard, N. C., Kurita, N., & Bird, M. I. (2016). Stable isotopic signature of Australian monsoon controlled by regional convection. *Quaternary Science Reviews*, 151, 228–235. <https://doi.org/10.1016/j.quascirev.2016.09.010>

## References From the Supporting Information

- Hersbach, H., Bell, B., Berrisford, P., Hirahara, S., Horányi, A., Muñoz-Sabater, J., et al. (2020). The ERA5 global reanalysis. *Quarterly Journal of the Royal Meteorological Society*, 146(730), 1999–2049. <https://doi.org/10.1002/qj.3803>
- Midhun, M., & Ramesh, R. (2016). Validation of  $\delta^{18}\text{O}$  as a proxy for past monsoon rain by multi-GCM simulations. *Climate Dynamics*, 46(5–6), 1371–1385. <https://doi.org/10.1007/s00382-015-2652-8>

- Nimya, S. S., Sengupta, S., Parekh, A., Bhattacharya, S. K., & Pradhan, R. (2022). Region-specific performances of isotope enabled general circulation models for Indian summer monsoon and the factors controlling isotope biases. *Climate Dynamics*, 59(11–12), 3599–3619. <https://doi.org/10.1007/s00382-022-06286-1>
- Pradhan, R., Singh, N., & Singh, R. P. (2019). Onset of summer monsoon in Northeast India is preceded by enhanced transpiration. *Scientific Reports*, 9(1), 18646. <https://doi.org/10.1038/s41598-019-55186-8>
- Sodemann, H., Masson-Delmotte, V., Schwierz, C., Vinther, B. M., & Wernli, H. (2008). Interannual variability of Greenland winter precipitation sources: 2. Effects of North Atlantic Oscillation variability on stable isotopes in precipitation. *Journal of Geophysical Research*, 113(D12), D12111. <https://doi.org/10.1029/2007JD009416>
- Stevens, B., Giorgetta, M., Esch, M., Mauritsen, T., Crueger, T., Rast, S., et al. (2013). Atmospheric component of the MPI-M Earth System Model: ECHAM6. *Journal of Advances in Modeling Earth Systems*, 5(2), 146–172. <https://doi.org/10.1002/jame.20015>
- Worden, J., Bowman, K., Noone, D., Beer, R., Clough, S., Eldering, A., et al. (2006). Tropospheric Emission Spectrometer observations of the tropospheric HDO/H<sub>2</sub>O ratio: Estimation approach and characterization. *Journal of Geophysical Research*, 111(D16), D16309. <https://doi.org/10.1029/2005JD006606>
- Worden, J., Kulawik, S., Frankenberg, C., Payne, V., Bowman, K., Cady-Peirara, K., et al. (2012). Profiles of CH<sub>4</sub>, HDO, H<sub>2</sub>O, and N<sub>2</sub>O with improved lower tropospheric vertical resolution from Aura TES radiances. *Atmospheric Measurement Techniques*, 5(2), 397–411. <https://doi.org/10.5194/amt-5-397-2012>
- Worden, J., Kulawik, S. S., Shephard, M. W., Clough, S. A., Worden, H., Bowman, K., & Goldman, A. (2004). Predicted errors of tropospheric emission spectrometer nadir retrievals from spectral window selection. *Journal of Geophysical Research*, 109(D9), D09308. <https://doi.org/10.1029/2004JD004522>
- Worden, J., Noone, D., Galewsky, J., Bailey, A., Bowman, K., Brown, D., et al. (2011). Estimate of bias in Aura TES HDO/H<sub>2</sub>O profiles from comparison of TES and in situ HDO/H<sub>2</sub>O measurements at the Mauna Loa observatory. *Atmospheric Chemistry and Physics*, 11(9), 4491–4503. <https://doi.org/10.5194/acp-11-4491-2011>